Concept of Cherenkov radiation sources based on complex surface structures for plasma science applications

W. Strachan, K. J. Wilson, K. Ronald, A. D. R. Phelps and A. J. MacLachlan

SUPA, Department of Physics, University of Strathclyde, Glasgow, United Kingdom

The concept is presented of high-power (kilowatt to megawatt) sub-THz and THz Cherenkov oscillators exploiting intricate two-dimensional periodic surface lattice (2D PSL) interaction cavities for the generation of coherent radiation. These sources can be tailored for diverse stationary and non-stationary regimes [1-6]. When operating in the steady-state regime, the sources are especially attractive for applications in plasma physics including enhanced plasma turbulence diagnostics and potentially as current drive sources for future fusion tokamaks [6]. A key advantage of these Cherenkov sources is that the operating frequency is primarily determined by the lattice parameters, rather than the magnetic field, enabling operation with modest axial guide fields.

Backward wave electron beam driven sources are traditionally designed with cavity diameters comparable to the radiation wavelength which ensures phase and spectral coherence but limits the output power at shorter wavelengths, with a typical $P \sim 1/f^2$ power scaling. The cylindrical interaction volume can be increased, while suppressing parasitic mode excitation, by introducing a shallow two-dimensional periodic sinusoidal corrugation along the cavity wall. The corrugation of a cylindrical 2D PSL (photographed in Figure 1) is defined as $r = R + \Delta r cos(\bar{m}\varphi)\cos(\bar{k}_z z)$ where R is the mean radius, Δr is the corrugation amplitude, $\bar{m}$ is the azimuthal order of the corrugation and $\bar{k}_z = \frac{2\pi}{d_z}$ is the lattice wavevector, determined by the axial period, d_z. The 2D corrugation supports the formation of a hybrid eigenmode composed of coupled volume and surface wave components, which under optimum operating conditions, becomes the dominant mode excited by the hollow annular electron beam.

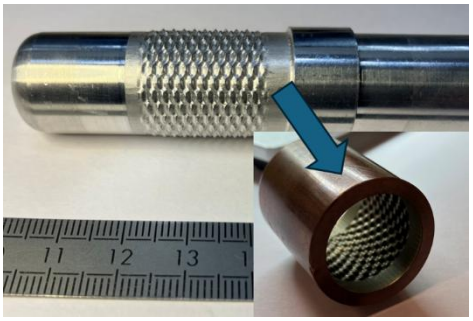

Figure 1: Photograph of 2D PSL (bottom) designed to operate at ~100 GHz, manufactured by copper electrodeposition onto a micromachined aluminum mandrel

The electromagnetic field structure inside a 2D PSL cavity is described by considering an equivalent smooth cylindrical waveguide of finite length excited by a fictitious magnetic surface current, $\boldsymbol{j}_m$.

This requires the following boundary constraint to be imposed:

$$\boldsymbol{j}_m = \boldsymbol{n} \times [\boldsymbol{\nabla}(r\boldsymbol{E} \cdot \boldsymbol{n})] + i\omega p \boldsymbol{n} \times [\boldsymbol{n} \times \boldsymbol{H}] \quad (1)$$

The transverse electric $\boldsymbol{E}$ and magnetic $\boldsymbol{H}$ fields are expanded as slowly varying wave packets with fast oscillating terms. The electric and magnetic fields are described as a summation of the

complete set of eigenmodes. Integrating the Poynting vector over the cylindrical cross section gives the power transmitted through the cavity. For the stationary, steady-state regime, where localized surface fields are coupled with a non-propagating (near cut-off) azimuthally symmetric $TM_{0,N}$ volume field, the wave equation is written:

$$\nabla_z^2 C_q^{v,s}(z) + \omega\delta C_q^{v,s}(z) \mp \frac{\bar{\omega}\Delta}{c^2} C_q^{v,s}(z) = N_{v,s} \oint \boldsymbol{j}_m . \boldsymbol{H}_q^* \, d\sigma \tag{2}$$

where $C_q^{v,s}$ is a slowly varying amplitude describing the gradual evolution of the volume and surface wave packets, δ is the Bragg detuning (which can be complex with the imaginary component describing losses) and $\bar{\omega}$ is the mean frequency of the volume and surface fields. The wave norm $N_{v,s}$ for the volume $(-)$ and surface fields $(+)$ is $N_{v,s} = i\omega\varepsilon_0 / \oint \boldsymbol{H}_q . \boldsymbol{H}_q^* \, d\sigma$, where $\boldsymbol{H}_q^*$ is the complex conjugate of the magnetic field of the eigenmode. Eq.(1) is substituted into the right-hand side of Eq.(2) which (for a non-trivial solution) must be non-zero. Averaging over the fast oscillation terms and renormalizing gives the following dispersion relation describing the coupled eigenmode of the 2D PSL [7]:

$$(\omega_e^2 - \Lambda^2)\{\Lambda^4 - 2\Lambda^2[(2 + \Gamma^2 + \omega_e^2) + (2 - \Gamma^2 + \omega_e^2)^2]\} = 2\alpha^4(2 - \Gamma^2 + \omega_e^2 - \Lambda^2) \tag{3}$$

where Λ is the normalized wave vector, ω_e is a variable angular frequency, $\omega_c^{v,s}$ is the angular cut-off frequency of the partial volume and surface modes, $\Delta\omega = \sqrt{((\omega_c^v)^2 + (\omega_c^s)^2)/2}$, $\Gamma = c\bar{k}_z/\Delta\omega$ is a geometrical detuning parameter, and α is the normalized coupling coefficient (defining the strength of the volume and surface field coupling).

The parameters of the 2D-PSL, designed to operate at 455GHz with a diameter D to wavelength λ ratio of D/λ =4.5, have been determined through an analytical dispersion study. The optimum parameters are: $R = 1.47$mm, $\bar{m} = 13$, $d_z = 0.30$mm and $\Delta r = 0.10$mm. Figure 2 shows the coupled dispersion (black curve) formed by the uncoupled partial volume (green curve) and surface (blue curve) modes. The red curve represents the beam line for a 117 kV electron beam, superimposed on the cold dispersion diagram to show the expected beam -wave interaction.

CST Particle Studio simulations of the 455GHz 2D PSL source, operating in the flat-top region of the lower dispersion branch, predict an output power of 2.6MW and electronic efficiency of 25%. Although a reduction in efficiency at high frequencies is expected due to increased ohmic losses associated with surface roughness, studies indicate that this can be somewhat mitigated through the implementation of a novel spent-electron energy recovery

scheme based on a multi-stage depressed collector [6,8,9].

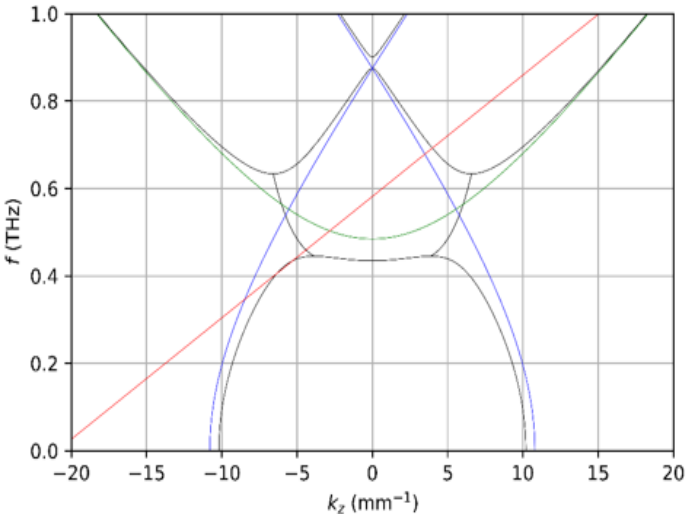

Figure 2: Coupled dispersion (black) of 2D PSL cavity. The green and blue curves are the uncoupled volume and surface field dispersions respectively. The red line represents a rectilinear electron beam with an accelerating voltage of 117kV

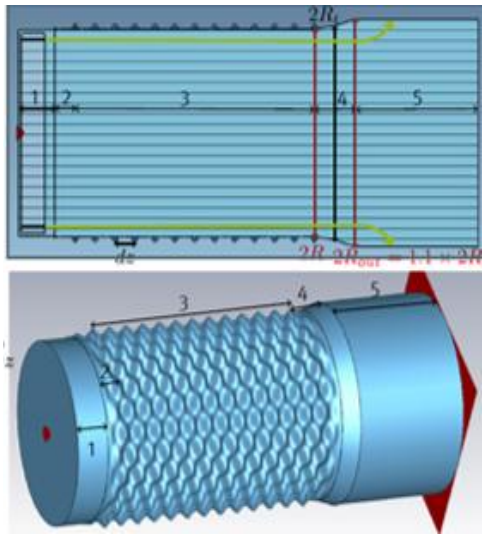

Figure 3: CST Studio Suite model of the 2D PSL source.

Particle-in-cell (PiC) studies of the 2D PSL sources demonstrate excellent spectral purity at the target frequency [4,5,6], confirming the utility of the 2D corrugation in providing mode selectivity for single-frequency operation in highly overmoded cavities. Furthermore, simulations indicate that it is possible to radiate nearly all the output power in a single high-order mode through careful consideration of the structure's geometry.

Figure 3 illustrates the CST Particle Studio model of the 2D PSL source. The electron injection scheme, comprising an accelerating potential applied to a planar cathode block via a discrete voltage port, is shown in region 1. In region 2, the corrugation amplitude is linearly tapered from 0 to Δr over one axial period. The 2D PSL interaction cavity is shown in region 3, where radiation is generated predominantly in the $HE_{13,1}$ mode (Figure 4) with a smaller fraction of the power in the azimuthally symmetric $TM_{0,N}$ modes. In region 4, the corrugation amplitude is linearly tapered from Δr to 0 while the mean radius is increased from r_0 to R_t over one axial period, giving a smooth transition to the cylindrical output waveguide (region 5). The taper is characterised by the intermediate radius R_t, a key design parameter that governs the modal power distribution at the output port.

Figure 5 shows the dependence of the output efficiency on the taper ratio, R_t/R, for operation in the dominant $HE_{13,1}$mode eigenmode. As the corrugation amplitude is reduced, tapers with smaller R_t/R ratios pass through a short section in which the $TE_{13,1}$and $TM_{0,5}$ modes fall below cut-off. This results in reflections back into the 2D PSL cavity, causing parasitic mode conversion into lower order $TM_{0,N}$ modes and a corresponding reduction in output efficiency. For larger taper ratios, the efficiency also decreases, likely due to increased impedance mismatch at the transition, which enhances reflections and reduces cavity loop gain.

Since hybrid modes are not supported in the smooth output waveguide, the $HE_{13,1}$eigenmode of the 2D PSL must transform into the $TE_{13,1}$ waveguide mode. Careful optimisation of the output taper minimises reflections and suppresses parasitic coupling into lower order $TM_{0,N}$ modes. For the optimum taper ratio of $R_t/R = 1.03$, PiC simulations predict that more than 99% of the total 2.6MW output power is radiated in the $TE_{13,1}$ mode.

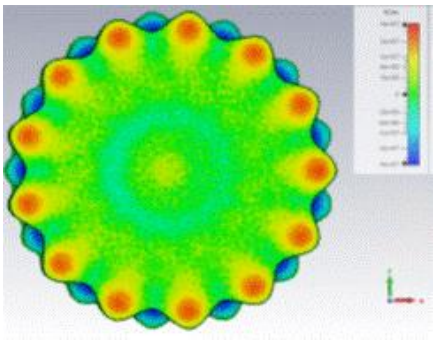

Figure 4: CST Particle Studio field contour plot illustrating the axial electric field component of the $HE_{13,1}$ hybrid coupled eigenmode.

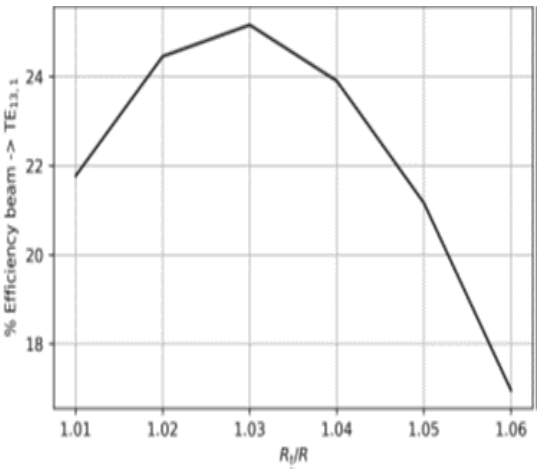

Figure 5: Effect of varying the taper ratio R_t/R on the output efficiency in the $TE_{13,1}$mode

In conclusion, the presented results demonstrate the potential of 2D PSL sources to deliver high-power, narrowband, short-pulse THz radiation. Their scalability in both frequency and transverse cavity dimensions makes them a promising approach to bridging the long-standing THz gap. The predicted combination of multi-megawatt peak power, excellent spectral purity, and high mode purity at 455 GHz offers significant potential for applications requiring intense coherent THz radiation, including next-generation high-resolution plasma diagnostics.

References

[1] I. V. Konoplev, A. J. MacLachlan, C. W. Robertson, A. W. Cross and A. D. R. Phelps, *Phys. Rev. A* 84, 013826 (2011).

[2] N. S. Ginzburg, A. M. Malkin, A. S. Sergeev and V. Y. Zaslavsky, *Appl. Phys. Lett.* 100, 143510 (2012).

[3] A. J. MacLachlan, A. D. R. Phelps, C. W. Robertson, P. MacInnes, C. G. Whyte and K. Ronald, *J. Plasma Phys.* 66, 125016 (2024).

[4] A. J. MacLachlan, C. W. Robertson, A. W. Cross and A. D. R. Phelps, *IEEE Trans. Electron Devices* 69, 6342–6347 (2022).

[5] A. J. MacLachlan, C. W. Robertson, A. W. Cross and A. D. R. Phelps, *IEEE Trans. Electron Devices* 70, 2760–2766 (2023).

[6] A. J. MacLachlan, L. Zhang, I. V. Konoplev, A. D. R. Phelps, C. W. Robertson, P. MacInnes, C. G. Whyte, K. Ronald, A. W. Cross and M. Henderson, *Sci. Rep.* 14, 23906 (2024).

[7] A. J. MacLachlan, C. W. Robertson, I. V. Konoplev, A. W. Cross, A. D. R. Phelps and K. Ronald, *Phys. Rev. Appl.* 11, 034034 (2019).

[8] UK Atomic Energy Authority and University of Strathclyde, L. Zhang, I. V. Konoplev, A. J. MacLachlan, K. Ronald, A. D. R. Phelps, C. G. Whyte, C. W. Robertson, P. MacInnes and A. W. Cross, GB Patent 2408675.3 (filed 17 June 2024).

[9] L. Zhang, W. He, A. W. Cross, A. D. R. Phelps, K. Ronald and C. G. Whyte, *IEEE Trans. Plasma Sci.* 37, 2328–2334 (2009).